PHYSICAL REVIEW D **93,** 115015 (2016)

New prospects in fixed target searches for dark forces with the SeaQuest experiment at Fermilab

S. Gardner[*]
Department of Physics and Astronomy, University of Kentucky, Lexington, Kentucky 40506-0055, USA

R. J. Holt[†]
Physics Division, Argonne National Laboratory, Argonne, Illinois 60439, USA

A. S. Tadepalli[‡]
Department of Physics and Astronomy, Rutgers University, Piscataway, New Jersey 08854, USA
(Received 13 September 2015; published 10 June 2016)

An intense 120 GeV proton beam incident on an extremely long iron target generates enormous numbers of light-mass particles that also decay within that target. If one of these particles decays to a final state with a hidden gauge boson, or if such a particle is produced as a result of the initial collision, then that weakly interacting hidden-sector particle may traverse the remainder of the target and be detected downstream through its possible decay to an e^+e^-, $\mu^+\mu^-$, or $\pi^+\pi^-$ final state. These conditions can be realized through an extension of the SeaQuest experiment at Fermilab, and in this initial investigation we consider how it can serve as an ultrasensitive probe of hidden vector gauge forces, both Abelian and non-Abelian. A light, weakly coupled hidden sector may well explain the dark matter established through astrophysical observations, and the proposed search can provide tangible evidence for its existence—or, alternatively, constrain a "sea" of possibilities.

DOI: 10.1103/PhysRevD.93.115015

I. INTRODUCTION

Searches for new physics have long been motivated by the seeming inadequacies of the Standard Model (SM). Some are theoretical and motivate searches for new physics at high-energy colliders, such as those that would help explain the origin of the weak scale, $v = (2\sqrt{2}G_F)^{-1/2} \approx 174$ GeV [1–3]. Others include its inabilities to explain either dark matter or dark energy and their relative predominance over visible matter in the cosmic energy budget, as deduced from astrometric observations [4–6]. The missing new physics can appear either at high energies and short-distance scales [7–10], or at low energies and long-distance scales [11–18]. Solutions to the dark matter problem could conceivably come from either source [19–23]. New long-distance effects are both possible and discoverable if the new light degrees of freedom couple to SM fields in a weak yet appreciable way. Such operators, or portals, to possible hidden sectors have been discussed extensively in the context of apparent cosmic and gamma ray anomalies, see e.g. Refs. [24–27], and have been proposed as an explanation of the muon $g-2$ anomaly [28]. [We also note earlier work in which a light U(1) gauge boson directly couples to SM fermions to explain the muon $g-2$ [29–31], as well as earlier astrophysical [32] anomalies.] In this paper we discuss the discovery prospects of an ultrasensitive broadband search for new long-distance physics, made possible through an extension of the SeaQuest E906 experiment at Fermilab.

The success of the SM in describing known particle phenomenology motivates a framework in which new physics appears as additions to the SM through effective operators $\mathcal{O}_i$ of mass dimension four or higher. The associated coupling constants are characterized by C_i/Λ^n, where $n \geq 0$, C_i is dimensionless, and Λ is the energy scale of new physics. As we have noted, these additions are thought to be either at high-energy scales for which $\Lambda > v$ [33–35] with $C \sim \mathcal{O}(1)$, or at low-energy scales for which $\Lambda \ll v$ or $n = 0$ with $C \ll \mathcal{O}(1)$. In the latter category, the most effort has been invested in operators for which $n = 0$, in part because their appearance does not usually require the inclusion of additional new physics to be theoretically consistent at high-energy scales [23]. Dark photon searches fall into this class. Higher-mass-dimension portals are also possible but have received much less attention. Their coupling to SM particles is expected to be much smaller, since $n > 0$. The experiment we consider, in which very small couplings can still be appreciable, thus serves as an ideal hunting ground for such effects.

Much experimental effort has been invested in searches for rare exotic particles through so-called beam dump experiments, in which detectors are mounted downstream of a particle beam stopped in a target. Our current

[*]gardner@pa.uky.edu
[†]holt@anl.gov
[‡]tadepalli@physics.rutgers.edu

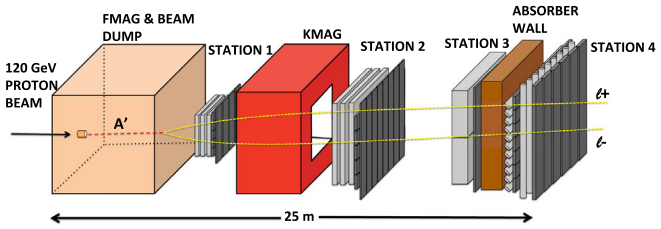

FIG. 1. Schematic of the SeaQuest spectrometer layout [36]. The 120 GeV proton beam from the Fermilab Main Injector approaches the spectrometer through a 25 cm–long hole of 2.5 cm in diameter in the 5 m–long solid iron magnet. An A' generated in the first meter of the beam dump traverses the focusing magnet (FMAG) without being affected by the magnetic field and can decay in the fiducial region into a lepton pair or a pion pair (upon upgrade). Stations 1, 2, and 3 comprise a series of drift chambers and an array of scintillator hodoscope paddles used for track reconstruction and triggering purposes. The 3 m–long air gap KTeV magnet (KMAG) is used to focus the muons back into the spectrometer to facilitate momentum measurements. The 1 m–long iron absorber wall is followed by an array of proportional tubes used for muon identification.

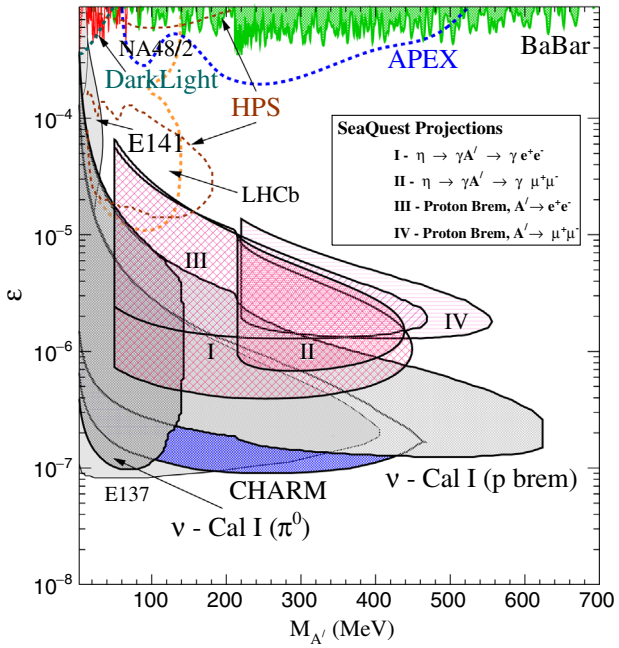

FIG. 2. Plot shows the projection contours of the coupling constant ε as a function of dark photon mass $m_{A'}$ for four different processes that could be used to search for dark photons at SeaQuest. Regions I and II are bounded by the contour plots for $\eta \to \gamma A' \to \gamma e^+e^-$ and $\eta \to \gamma A' \to \gamma\mu^+\mu^-$, respectively, whereas regions III and IV refer to the limits inferred from use of the proton bremsstrahlung production mechanism, followed by $A' \to e^+e^-$ (III) and $A' \to \mu^+\mu^-$ (IV) decay. The area excluded by electron beam dump experiments E137 [37,40] and E141 [41], and the searches by *BABAR* [50], CHARM [43,44], and NA48/2 [47] are bounded by solid lines at 90% C.L., whereas those excluded by ν-Cal I (π^0) [51] and ν-Cal I (p-Brem) [52] are bounded by solid lines at 95% C.L. Also, the planned sensitivities of APEX (full run) [56], HPS [57,58], DarkLight [59] (all at 90% C.L.) and LHCb [66] (at 95% C.L.) are shown as dotted lines for comparison. We omit the anticipated limits from VEPP-3 [60], Refs. [62,63], Mu3e [64], and MESA [61], which all probe lighter masses, as well as Ref. [65], for visual clarity. The region above $\varepsilon = 10^{-3}$ (not shown in the figure) has been excluded by several experiments such as E774 [42], APEX (test run) [45], HADES [67], KLOE [46], PHENIX [48], and MAMI [49], along with the 2σ exclusion limit obtained from $(g-2)_e$ [68]. Approximate limits at still weaker mixing angles from the LSND experiment [38,69,70] and from astrophysical considerations [37,71–75] have been omitted. Note that the limits shown all assume that decays of the A' to the invisible sector are nonexistent.

investigation concerns the discovery prospects of an experiment of this class, and a schematic is shown in Fig. 1. As emphasized by Ref. [37], the potential parameter space for a dark photon—or, indeed, for any particle probed via a $n = 0$ connector—is vast, in both candidate mass and mixing angle. Beam dump experiments that involve displaced vertices for dark photon production and decay are largely sensitive to small mixing angles, with electron and proton beam dump experiments giving comparable constraints [37]. Dedicated efforts have been made to address the remaining holes in parameter space [37–39], with many recently completed searches and reanalyses of earlier ones [37,40–55] and many more proposed and under development [56–66].

The extension of the SeaQuest experiment we consider can contribute to this effort in different ways. Not only can it probe new regions of dark photon parameter space, leading either to a dark photon discovery or a refinement of that phase space, but it can also be used to probe dark forces that enter solely through their mixing with QCD degrees of freedom. In this latter case, proton beam dump experiments play a special role, particularly if the downstream spectrometer can detect pions. In what follows, we expound on the discovery prospects of the experiment shown in Fig. 1. For reference, the manner in which the existing SeaQuest spectrometer can contribute to a dark photon search, with reference to efforts under development worldwide, is shown in Fig. 2. We note that the SeaQuest experiment can probe part of the dark photon parameter space to be probed by the SHiP experiment at CERN [65]. We also consider the discovery prospects associated with a spectrometer upgrade to permit electron and pion detection.

We now sketch the content of the sections to follow. We begin with an overview of hidden portal models, highlighting, in particular, the various ways in which quark and gluon degrees of freedom can also play a role. We then proceed to describe the specific manner in which hidden portals can be probed at SeaQuest. In this initial investigation we place a particular focus on the radiative decays of the light mesons π^0 and η. We expect light mesons to be

produced copiously in a proton beam dump experiment [76], and their radiative decays are controlled by the chiral anomaly even if the final state contains strongly interacting particles. The proton bremsstrahlung contour for SeaQuest in Fig. 2 was produced by following the method outlined in Ref. [52] and the simulation techniques described in Sec. IV A. Finally, we turn to a discussion of the experimental prospects, illustrating concretely how SeaQuest can probe dark forces, before offering our concluding summary.

II. HIDDEN-SECTOR PORTALS

The known interactions and particle content of the SM are richly complicated, and this itself suggests that the bulk of the matter content in the Universe should be similarly complex. Existing constraints on its content, however, are minimal. Nevertheless, the observation that dark matter is stable over at least Gyr time scales begs an explanation, and it is natural to think that a gauge symmetry of the hidden sector can provide it. The matter content of such a hidden sector need only interact gravitationally with the matter we know—no other interactions are required, though it has become popular in recent years to build theoretical models of cosmogenesis that tie the generation of dark matter with that of the cosmic baryon asymmetry, solving two problems at once [77–79]. Although the existence of hidden-sector gauge interactions could potentially impact the morphology of dwarf galaxies [80] and have other observational consequences [81–84], the ability to discover such hidden sectors may rest on the manner in which they can connect to the particles and interactions of the SM.

It has been popular to consider portals that consist of operators that do not require new high-energy physics for theoretical consistency, so that $n = 0$, or less. An economical summary of such portals [23,38] is

$$\mathcal{L}_{n\leq 0} = \kappa B^{\mu\nu} V_{\mu\nu} - H^\dagger H(AS + \lambda S^2) - Y_N LHN, \quad (1)$$

where $B^{\mu\nu}$ is the field-strength tensor associated with $\mathrm{U}(1)_Y$ in the SM, H is the SM Higgs field, and L is a SM left-handed (lepton) doublet. The explicit hidden-sector degrees of freedom are a field-strength tensor $V_{\mu\nu}$ associated with a hidden U(1) symmetry, a scalar S, and a fermion N. These new degrees of freedom can couple to further hidden-sector degrees of freedom, and the latter can be richly diverse.

The new gauge boson degrees of freedom can be dark photons or Z's, or both, depending on the manner in which their mass is generated [68,85]. If the dark photon is massless, kinetic mixing with the visible photon would engender a DM electric charge [86], and the resulting constraints can be severe [80,87,88], though they can also be weakened, either by introducing multiple species with a net dark matter electric charge of zero [89] or by making the dark-matter particle a (nearly) electrically neutral composite [81,82,90,91]. The latter, "dark atom" scenarios possess an additional length scale whose existence is also constrained by cosmic microwave background (CMB) observations [92]. In this paper we focus on hidden vector gauge bosons that range from some 10 MeV to 700 MeV in mass, for which the noted astrophysical constraints do not operate. We note in passing, however, that extremely weakly coupled dark photons with such mass scales are nevertheless constrained by supernova cooling [37], as well as CMB and Big Bang nucleosynthesis (BBN) [73] considerations. A minimal enlargement of the SM in the presence of hidden gauge bosons is of the form [37–39]

$$\mathcal{L} = \mathcal{L}_{\mathrm{SM}} + \frac{1}{2}\kappa B^{\mu\nu} V_{\mu\nu} - \frac{1}{4} V_{\mu\nu} V^{\mu\nu} + \frac{1}{2} m_{A'}^2 A'^{\mu} A'_{\mu}, \quad (2)$$

where $V_{\mu\nu} = \partial_\mu A'_\nu - \partial_\nu A'_\mu$. The kinetic mixing term $B^{\mu\nu} V_{\mu\nu}$ engenders, upon diagonalization and field redefinition, a photon with an A' admixture controlled by the small parameter κ. Specifically, $A^\mu \to A^\mu - \varepsilon A'^\mu$, where $\varepsilon \equiv \kappa \cos\theta_W$. In contrast, mixing with the Z is suppressed by a nominally large ratio of masses, namely by $\mathcal{O}(\varepsilon m_{A'}^2/M_Z^2)$ [37,85,93]. However, with an enlarged Higgs sector, such as in the two-Higgs-doublet model, mixing with both the photon and Z can occur, and the candidate dark gauge boson becomes a dark Z or "Z_d" [68,85,94,95]. In this case, after diagonalization of the kinetic mixing term, the photon and Z acquire a small admixture of Z_d which couples to SM electromagnetic and weak-neutral currents as per [68,85,94,95]

$$\mathcal{L}_{\text{dark Z}} = -\left(\varepsilon e J^\mu_{\mathrm{em}} + \varepsilon_Z \frac{g}{2\cos\theta_W} J^\mu_{\mathrm{NC}}\right) Z_{d\mu}, \quad (3)$$

with the earlier dark photon model emerging in the $\varepsilon_Z = 0$ limit. The appearance of $Z - Z_d$ mixing gives rise to low-energy parity-violating effects as well [68,85,95]. Nevertheless, it is apparent that dark photon searches also restrict the Z_d.

Thus far we have considered kinetic mixing models associated with an Abelian gauge symmetry. The gauge boson mass, be it that of A' or Z_d, can be arranged through a Stueckelberg mechanism [96,97], but it can also be generated though a SM Higgs mechanism in the hidden sector [24,98].[1] The discovery of a massive Abelian gauge boson can thus implicitly hint at the existence of non-Abelian hidden-sector interactions as well. Non-Abelian interactions can also appear explicitly, and we now delve into this possibility directly and consider, in particular, how QCD degrees of freedom can serve as a portal to a possible hidden sector.

It has long been thought that new matter with QCD-like interactions could exist [99–101], though the internal color symmetry of QCD would seem to preclude vector portals of

[1]The hidden scalar can also function as a portal to the hidden sector, as per Eq. (1).

the sort we have considered thus far. Nevertheless, portals with QCD degrees of freedom need not yield higher mass-dimension operators, nor do they necessarily require new UV degrees of freedom for theoretical consistency. We highlight some of the possibilities in what follows. We loosely organize our discussion in terms of portals of increasing mass dimension, beginning with portals arising from a gauged baryon vector current and then turning to portals employing multiquark operators and gluons.

The possibility of a light U(1) gauge boson B associated with a gauged baryon vector current is a notion of some standing [102–111], though much of its focus has concerned the consequences of its kinetic mixing with the $U(1)_Y$ sector of the SM [106–108]. Recently Tulin [110] has noted the possibility of a mass-dimension-four connector in terms of quarks, namely

$$\mathcal{L}_{\mathrm{B}} = \frac{1}{3} g_B \bar{q} \gamma^\mu q B_\mu, \tag{4}$$

where B_μ is the new gauge field that couples to baryon number. Since $U(1)_B$ is anomalous in the SM, its mixing with SM fields requires new UV degrees of freedom for theoretical consistency [23,102,110,111], though such constraints have been successfully implemented—note, e.g., Refs. [103–105,109,111]. Since the gauge coupling g_B is universal for all quarks, the B is taken to be strictly isoscalar, so that $B \to \pi^+\pi^-$ does not occur if G parity is not violated [110]. For B bosons in the mass window of $M_\pi \lesssim M_B \lesssim 620$ MeV, the primary decay mode is thus $B \to \pi^0\gamma$. Mixing of the B with the photon can appear through radiative corrections [106–108], so that $B \to \ell^+\ell^-$ can occur as well. The B can be probed through the radiative decays of the light mesons [102,110]. A distinct signature of this particular model is the appearance of $B \to \pi^0\gamma$ decay, a final state which the SeaQuest spectrometer cannot detect. Limits on the A', however, translate to those on B in a model-dependent way [110]. It is worth noting, however, that the B need not be strictly isoscalar. As established from phenomenological studies of the nucleon-nucleon force, both the ρ and ω mesons couple to the baryon vector current because the nucleon-nucleon force is not charge independent, though the coupling of the ω is roughly a factor of 5 larger than that of the ρ [112]. Generalizing Eq. (4) to the form

$$\mathcal{L}_{\mathrm{B}'} = g^u_{B'} \bar{u} \gamma^\mu u B'_\mu + g^d_{B'} \bar{d} \gamma^\mu d B'_\mu + \ldots, \tag{5}$$

we term this gauge boson B' and relegate the contributions of other quarks to the ellipsis. Thus, $B' \to \pi^+\pi^-$ can occur without breaking G parity, as had been assumed in Ref. [102]. The B' can be probed through the decay $\eta \to B'\gamma \to \pi^+\pi^-\gamma$, which is accessible at SeaQuest. Other models can be probed in this manner as well. For example, in the model of Dobrescu and Frugiuele [111], the gauge boson that couples to baryon number is a leptophobic Z', where the interactions of the Z' with quarks, for the first generation, are of the form

$$\mathcal{L}_{\mathrm{qZ}'} = \frac{g_z}{2} (z_Q \bar{Q}_L \gamma^\mu Q_L + z_u \bar{u}_R \gamma^\mu u_R + z_d \bar{d}_R \gamma^\mu d_R) Z'_\mu. \tag{6}$$

The field Q_L is a left-handed quark doublet, and u_R and d_R are right-handed singlets—we see that the Z' can couple to isovector combinations of quarks as well.

We now turn to the possibility of portals comprised of operators of mass dimension greater than four. The existence of such operators can require the existence of new UV physics for theoretical consistency, but this does not negate them as a possibility. In this case, it is possible to connect to non-Abelian hidden-sector degrees of freedom directly. Starting in dimension six, we note the following possibilities,[2] namely

$$\frac{\kappa'}{\Lambda^2} (\bar{q}_{L(R)} \gamma_\mu q_{L(R)}) (\bar{q}'_{L(R)} \gamma^\mu q'_{L(R)}), \tag{7}$$

where q' is a hidden-sector quark, admitting the possibility of a hidden-sector "pion" [38], e.g., for which dark matter models have recently been developed [114,115]. We note Refs. [116,117] as alternate models of non-Abelian hidden sectors. Explicitly non-Abelian portals also appear, such as [98]

$$\frac{\kappa'}{\Lambda^2} \mathrm{tr}(\Phi^a F^a_{\mu\nu}) \mathrm{tr}(\tilde{\Phi}^b \tilde{F}^{b\mu\nu}), \tag{8}$$

where $F^{a\mu\nu}$ is the QCD field-strength tensor and $\tilde{F}^{b\mu\nu}$ denotes an analogous non-Abelian object, though it need not reside in a theory of SU(3) color. Note that the appearance of new heavy degrees of freedom is also explicit through that of the heavy scalars Φ and $\tilde{\Phi}$ that transform under the adjoint representations of their respective groups [98]. Finally, in dimension eight, it is also possible to have a pure glue-glue connector

$$\mathrm{tr}(F^{a\mu\nu} F^a_{\mu\nu}) \mathrm{tr}(\tilde{F}^b_{\delta\rho} \tilde{F}^{b\delta\rho}), \tag{9}$$

which has also served as the basis for "hidden valley" models [118] that can possess striking collider signatures [118–121]. This connector is also noteworthy as an UV "complete" extension of the SM. That is, operators with mass dimension greater than four that break no SM symmetries do not require additional UV physics to be viable, an idea exploited in the dark matter model of Ref. [117].

The various higher mass dimension connectors we have discussed appear in connection with QCD couplings, so

[2]We note, however, that axion degrees of freedom can connect to SM fermions in dimension five [38], though their couplings to quarks are constrained by BBN [113].

that "infrared slavery" at low energy can partially offset the ratio of mass scale suppression associated with their higher mass dimension. Indeed, at low energies we should recast the connectors we have considered in terms of hadronic degrees of freedom. A pertinent model is provided by the hadronic kinetic mixing model of Ref. [122], which is based on the hidden local symmetry model of QCD [123,124], in which the ρ mesons function as effective gauge bosons of the strong interaction, and on vector-meson dominance [125,126]. That is [122],

$$\mathcal{L}_{\rm mix} = -\frac{1}{4}\rho^a_{\mu\nu}\rho^{a\mu\nu} - \frac{1}{4}\rho'^a_{\mu\nu}\rho'^{a\mu\nu} + \frac{\varepsilon}{2}\rho^a_{\mu\nu}\rho'^{a\mu\nu} + \frac{m_\rho^2}{2}\rho^a_\mu\rho^{a\mu} + \frac{m_{\rho'}^2}{2}\rho'^a_\mu\rho'^{a\mu} + \kappa_\rho J^{\mu a}\rho^a_\mu, \tag{10}$$

where $J^{a\mu}$ denotes the hadronic vector current and $\rho^{(\prime)a}$ are the gauge bosons of a hidden local SU(2) symmetry with $\rho^{(\prime)a}_{\mu\nu} = \partial_\mu\rho^{(\prime)a}_\nu - \partial_\nu\rho^{(\prime)a}_\mu$ [126]. This model resembles the dark photon models discussed earlier but contains two massive vector fields; its possible footprints at low energies, in beta decay, have been considered by Gardner and He [122]. The kinetic mixing terms can be removed through the field redefinition $\rho^a_\mu \to \rho^a_\mu - \varepsilon\rho'^a_\mu$, thus yielding a coupling of the hadronic vector current to ρ'^a. Here the ρ'^0 can be probed at SeaQuest. Indeed, all the quark-level models we have considered that permit a hidden-sector contribution to a $\pi^+\pi^-$ final state can feed the low-energy constant ε in Eq. (10). In this sense a ρ' search is rather generic, as it constrains the B', leptophobic Z', and higher-dimension QCD connectors we have considered as well.

III. PROBING HIDDEN SECTORS AT SEAQUEST

Enormous numbers of light mesons would be produced in the collision of an intense 120 GeV proton beam with a thick iron target, and we propose to search for the light hidden-sector particles that may be produced through their decays. Moreover, dark gauge bosons can be produced directly through initial-state radiation from a high-energy proton beam, followed by a hard proton-iron collision; here we employ the formalism of Ref. [52].

The models discussed in the previous section can all be probed through an extension of SeaQuest, though the distinctive features of a dark Z—its ability to mediate parity violation—would not be apparent. Nevertheless, sensitivity to a parity-violating dark gauge boson (Z_d) should result from the use of a polarized proton beam [127] via the initial-state radiation production mechanism.[3] Specifically, the Z_d can be produced via either a vector or axial-vector coupling. These processes can interfere to give different $\ell^+\ell^-$ yields as a function of the beam helicity.

Irrespective of such developments, searches for hidden dark forces in atomic parity violation, as well as in parity-violating electron scattering, play an important complementary role [95].

The following decay chains are examples of processes that can be studied at SeaQuest. We note that A' searches automatically limit the Z_d as well.

(1) $\pi^0 \to \gamma A' \to \gamma e^+e^-$: to search for A'.
(2) $\eta \to \gamma A' \to \gamma\ell^+\ell^-$ *with* $\ell \in e,\mu$: to search for A'. The ability to detect different lepton final states offers the possibility of testing the kinetic mixing mechanism.
(3) $\eta \to \gamma A' \to \gamma\pi^+\pi^-$: to search for A'—or ρ', a "strongly" interacting hidden sector gauge boson. The presence of the ρ' would be signaled if no accompanying events were observed in $\ell^+\ell^-$.
(4) *proton bremstrahlung of* A' *with* $A' \to \ell^+,\ell^-$ *and* $\ell \in e,\mu$ *or* $A' \to \pi^+\pi^-$: to search for A'. Study of $A' \to \pi^+\pi^-$ also permits a search for a leptophobic dark gauge boson Z' [111].
(5) *Drell-Yan production of* A' *with* $A' \to \ell^+,\ell^-$ *and* $\ell \in e,\mu$: to search for A'—studying the possibility of $A' \to \pi^+\pi^-$ also opens sensitivity to a leptophobic dark gauge boson. This perturbative QCD mechanism for dark gauge boson production is under study [128].

Although we focus on the possibility of new vector gauge forces in this paper, we wish to emphasize that the discovery prospects of the type of search we discuss span a much broader horizon. We note that the study of light meson decays in this context includes these additional possibilities.

(1) $\eta \to \pi^0 h_d \to \pi^0\pi^+\pi^-$: to search for a dark Higgs h_d, noting Refs. [129,130], as well as for scalar dark matter that mixes with QCD gluons [117].
(2) $K^\pm \to \pi^\pm Z_d \to \pi^\pm\ell^+\ell^-$ *with* $\ell \in e,\mu$: to search for Z_d [95].

We now evaluate each of the radiative decay processes in turn.

A. The decay $\pi^0 \to \gamma A' \to \gamma\ell^+\ell^-$

The decay amplitude $\pi^0 \to \gamma\gamma^{(*)}$ is controlled by the primitive axial anomaly [131,132], even if QCD corrections that would alter its form only vanish for on-mass-shell photons [133]. Consequently, the partial width for Dalitz decay is usually normalized relative to that for $\pi^0 \to \gamma\gamma$ [134–136]. To validate our procedures, we begin by computing the partial width for Dalitz decay at tree level in the SM [134–136], which yields, after a partial integration over the three-body phase space,

[3]Parity violation could be studied through the use of either a polarized beam or an exceptionally long polarized target, but the latter is not planned for the extension of the SeaQuest experiment we consider here.

$$\Gamma(\pi^0 \to \gamma e^+ e^-) = \frac{2\alpha\Gamma_0}{3\pi}\int_{r^2}^1 dx |f(1,0,x)|^2 \frac{(1-x)^3}{x} \times \beta\left(1+\frac{r^2}{2x}\right), \tag{11}$$

where $\Gamma_0 \equiv \Gamma(\pi^0 \to \gamma\gamma)$, $x = s/M_{\pi^0}^2$, $r = 2m_e/M_{\pi^0}$, $\beta = \sqrt{1-r^2/x}$, and s is the invariant mass of the e^+e^- pair. We note that $f(1,0,x)$ is the $\pi^0 \to \gamma\gamma^*$ transition form factor [noting $f(p^2/M_{\pi^0}^2, k_1^2/M_{\pi^0}^2, k_2^2/M_{\pi^0}^2)$ for $\pi^0(p) \to \gamma^*(k_1)\gamma(k_2)$ decay [135]], where $f(1,0,0) = 1$ appears in $\pi^0 \to \gamma\gamma$. The transition form factor has been studied extensively because of its connection to the analysis of the hadronic light-by-light contribution to the anomalous magnetic moment of the muon, $g-2$, and a model-independent representation, based on Padé approximates, of the transition form factor data from CELLO, CLEO, *BABAR*, and Belle, yields

$$f(1,0,x) = 1 + a_\pi x + b_\pi x^2 + \mathcal{O}(x^3), \tag{12}$$

with $a_\pi = 0.0324(12)_{\rm stat}(19)_{\rm sys}$ and $b_\pi = (1.06(9)_{\rm stat}(25)_{\rm sys}) \times 10^{-3}$ [137], though a dispersive approach yields similar results with smaller errors: $a_\pi = 0.0307(6)$ and $b_\pi = (1.10(2)) \times 10^{-3}$ [138]. For reference, an analysis of $\pi^0 \to \gamma e^+ e^-$ in two-flavor chiral perturbation theory (ChPT) enlarged by electromagnetism yields $a_\pi = 0.029(5)$ [136], whereas ChPT at one loop with $\mu = m_\rho$ yields $a_\pi = 0.036$ [139]. Computing $\Gamma(\pi^0 \to \gamma e^+ e^-)/\Gamma_0$ from Eq. (11) using empirical inputs from Ref. [140] yields 1.185×10^{-2} if the transition form factor is set to 1, in agreement with Refs. [134,136]. Including $f(1,0,x)$ using the central values of Ref. [137] yields 1.188×10^{-2}, whereas the experimental result $\Gamma(\pi^0 \to e^+e^-\gamma)/\Gamma_0 = (1.188(30)) \times 10^{-2}$ [140]. We conclude that our framework works very well. The three-body partial width via an A' intermediate state follows from inserting the factor

$$\frac{x^2}{((x-x_{A'})^2 + x_{A'}\tilde{\Gamma}_{A'}^2)}\varepsilon^4 \tag{13}$$

under the phase-space integral, where $x_{A'} = m_{A'}^2/M_\pi^2$ and $\tilde{\Gamma}_{A'} = \Gamma_{A'}/M_\pi$, to yield

$$\Gamma(\pi^0 \to \gamma A' \to \gamma e^+ e^-) = \Gamma_0 \int_{r^2}^1 dx \frac{\alpha}{\pi}\varepsilon^4 |f(1,0,x)|^2 \times \frac{2(1-x)^3 x}{((x-x_{A'})^2 + x_{A'}\tilde{\Gamma}_{A'}^2)}\beta\left(1+\frac{r^2}{2x}\right). \tag{14}$$

Existing searches for hidden gauge bosons, such as A' and Z_d, have presumed that there are no lighter particles within the hidden sector, so that these particles decay only to SM particles. In this case, this implies $\mathcal{B}(A'(Z_d) \to e^+e^-) = 1$. Consequently, since $\tilde{\Gamma}_{A'} \sim \alpha\varepsilon^2 \ll 1$, we can employ the narrow width approximation, replacing

$$((x-x_{A'})^2 + x_{A'}\tilde{\Gamma}_{A'}^2)^{-1} \to \frac{\pi}{\sqrt{x_{A'}}\tilde{\Gamma}_{A'}}\delta(x-x_{A'}) \tag{15}$$

to yield

$$\Gamma(\pi^0 \to \gamma A' \to \gamma e^+ e^-) = |f(1,0,x_{A'})|^2 \Gamma(\pi^0 \to \gamma A') \times \mathcal{B}(A' \to e^+e^-), \tag{16}$$

where

$$\Gamma(\pi^0 \to \gamma A') = 2\varepsilon^2\left(1-\frac{m_{A'}^2}{M_\pi^2}\right)^3 \Gamma_0 \tag{17}$$

and

$$\Gamma(A' \to e^+e^-) = \frac{1}{3}\alpha\varepsilon^2 m_{A'}\sqrt{1-4\frac{m_e^2}{M_{A'}^2}}\left(1+2\frac{m_e^2}{m_{A'}^2}\right). \tag{18}$$

We note $\Gamma_{A'} = \Gamma(A' \to e^+e^-)$ by assumption. As a result, Eq. (16) can be viewed as the product of two sequential two-body decays, in which the A' appears on its mass shell, moderated by the π^0 transition form factor. If, rather, $x_{A'} > 1$, then the integral in Eq. (14) is regular even if $\Gamma_{A'} = 0$. We set this possibility aside, however, both here and in what follows, because an on-mass-shell particle is needed to evaluate its transit through the iron beam stop. It is worth emphasizing that the transition form factor we have noted in Eq. (12) is developed for the low-momentum transfer regime $x \ll 1$, whereas $x_{A'}$ can be of $\mathcal{O}(1)$. Using a Padé approximate of $P_3^2(s)$ form [137],[4] which satisfies the asymptotic limit from perturbative QCD [142] for the transition form factor, we have checked that for our application its numerical effects are so slight that we can neglect it with impunity.

B. The decay $\eta \to \gamma A' \to \gamma \ell^+ \ell^-$

To evaluate $\eta \to \gamma\ell^+\ell^-$ decay in the SM, we need only replace $M_\pi \to M_\eta$ and $m_e \to m_\ell$ in Eq. (11) and modify the transition form factor. A new parametrization [143] of the $\eta \to \gamma^*\gamma$ form factor, including the latest measurement of $\eta \to e^+e^-\gamma$ [144], and employing rational approximates [145], has recently become available. With $x \to s/M_\eta^2$, and as $x \to 0$ (with $x > 0$), we have

$$f_\eta(1,0,x) = 1 + b_\eta x + c_\eta x^2 + d_\eta x^3 + \mathcal{O}(x^4), \tag{19}$$

[4]We thank P. Masjuan for graciously providing it to us [141].

where $b_\eta = 0.576(11)_{\rm stat}(4)_{\rm sys}$, $c_\eta = 0.339(15)_{\rm stat}(5)_{\rm sys}$, and $d_\eta = 0.200(14)_{\rm stat}(18)_{\rm sys}$ [143]. Since the integral of Eq. (11) includes $x = 1$ as well, we also evaluate $f_\eta(1,0,x)$ using the complete rational approximate,[5] noting that time-like data is available up to $s \approx 0.22$ GeV^2 [143]. Employing Eqs. (11) and (19) to compute $\Gamma(\eta \to \gamma e^+ e^-)/\Gamma_0^\eta$ yields 1.67×10^{-2} (and 1.62×10^{-2} without the form factor) to compare with the experimental ratio $1.75(06) \times 10^{-2}$ [140]. Computing, rather, $\Gamma(\eta \to \gamma \mu^+ \mu^-)/\Gamma_0^\eta$ yields 8.17×10^{-4} (and 5.51×10^{-4} without the form factor) to compare with the experimental ratio $7.87(13) \times 10^{-4}$ [140]. Using the complete rational approximate makes for little impact, changing only the value of $\Gamma(\eta \to \gamma \mu^+ \mu^-)/\Gamma_0^\eta$ result to 8.19×10^{-4} once the empirical central value of $\Gamma_0^\eta \equiv \Gamma(\eta \to \gamma\gamma)$ is imposed. The estimates we have made agree with the experimental central values at the ≈5% level, a disagreement larger than one would naively expect from radiative corrections but which, rather, appears to stem from differences in recent experimental results for $\Gamma(\eta \to e^+ e^- \gamma)$ [144,146] and the world average [140]. It is worth noting that the η decay partial widths are measured relative to Γ_0^η, and although a recent precision measurement of Γ_0^η exists [147], differences in measurements of Γ_0^η from the e^+e^- collisions and electron-nucleus scattering, through use of the Primakoff effect, impact earlier determinations of the partial widths [140]. Irrespective of this, we conclude that our framework certainly works sufficiently well for our current purpose. Turning to the possibility of an A' intermediate state, we update Eq. (14) to

$$\begin{aligned}\Gamma(\eta \to \gamma A' \to \gamma \ell^+ \ell^-) &= \Gamma_0^\eta \int_{r_\ell^2}^1 dx \frac{\alpha}{\pi} \varepsilon^4 |f_\eta(1,0,x)|^2 \\ &\times \frac{2(1-x)^3 x}{((x - x_{A'})^2 + x_{A'} \tilde{\Gamma}_{A'}^2)} \beta \left(1 + \frac{r_\ell^2}{2x}\right), \end{aligned} \tag{20}$$

where $M_{\pi^0} \to M_\eta$, $r_\ell = 2m_\ell/M_\eta$, and $\beta = \sqrt{1 - r_\ell^2/x}$. Here, too, we can use the narrow width approximation to find

$$\begin{aligned}\Gamma(\eta \to \gamma A' \to \gamma \ell^+ \ell^-) &= |f_\eta(1,0,x_{A'})|^2 \Gamma(\eta \to \gamma A') \\ &\times \mathcal{B}(A' \to \ell^+ \ell^-), \end{aligned} \tag{21}$$

where $\Gamma(\eta \to \gamma A')$ and $\Gamma(A' \to \gamma \ell^+ \ell^-)$ follow from suitable substitutions in Eqs. (17) and (18).

[5]We thank the authors of Ref. [143] for a high-precision version of the function $P_1^7(Q^2)$ that appears in their Table 5, making it suitable for numerical work [141,143].

C. The decay $\eta \to \gamma A' \to \gamma \pi^+ \pi^-$

To study this particular channel, we need only compute $\Gamma(A' \to \pi^+ \pi^-)$, replacing ℓ with π in Eq. (21). Recalling the definition of the π form factor $F_\pi(s)$ in $e^+e^- \to \pi^+\pi^-$ at center-of-mass energy $\sqrt{s}$ [148], we note the decay amplitude is of the form

$$\mathcal{M}(A'(p) \to \pi^+(p_1)\pi^-(p_2)) = \varepsilon e \varepsilon_{A'}^\mu (p_1 - p_2)_\mu F_\pi(p^2), \tag{22}$$

so that the decay width is

$$\Gamma(A' \to \pi^+ \pi^-) = \frac{1}{12} \varepsilon^2 \alpha m_{A'} \left(1 - 4\frac{M_\pi^2}{m_{A'}^2}\right)^{3/2} |F_\pi(m_{A'}^2)|^2. \tag{23}$$

This can be compared to the estimate used earlier in the literature [37,52],

$$\Gamma(A' \to \text{hadrons}) = \frac{1}{3} \varepsilon^2 \alpha m_{A'} \mathcal{R}(m_{A'}^2), \tag{24}$$

where the cross-section ratio

$$\mathcal{R}(s) \equiv \frac{\sigma(e^+e^-(s) \to \text{hadrons})}{\sigma(e^+e^-(s) \to \mu^+\mu^-)} \tag{25}$$

below the $\pi\omega$ threshold evaluates to

$$\mathcal{R}(s) = \frac{1}{4} \frac{(s - 4M_\pi^2)^{3/2} |F_\pi(s)|^2}{(s - 4M_\mu^2)^{1/2}(s + 2M_\mu^2)}, \tag{26}$$

revealing that Eq. (24) is a very good approximation over a large mass range—only the factor $(1 - 4M_\mu^2/s)^{1/2}(1 + 2M_\mu^2/s)$ is extraneous. A simple form of F_π especially suitable for $\sqrt{s} \lesssim 600$ MeV is [149]

$$F_\pi(s) = \frac{-f_{\rho\gamma} g_\rho}{s - M_\rho^2 + i\Pi(s)}, \tag{27}$$

where $\Pi(s) = (M_\rho^2/\sqrt{s})(p(s)/p(M_\rho^2))^3 \Gamma_\rho$ includes a running ρ width, with $p(s) = \sqrt{s/4 - M_\pi^2}$ and a normalization as per Ref. [150]. An explicit test of this form is shown in Fig. 5 of Ref. [150], for which $f_{\rho\gamma} = 0.122(1)$ GeV^2 [151], $g_\rho = 5.8$, $M_\rho = 769.3$ MeV and $\Gamma_\rho = 150$ MeV are used. The ρ is a broad resonance, and if its mass and width are determined as per the real-axis prescription of Eq. (27), with an s-dependent width, as distinct from the location of its pole in the complex plane, then the resulting resonance parameters depend on the precise form of $F_\pi(s)$ [148,151]. Such a real-axis prescription is employed in the determinations averaged by Ref. [140], for which $M_\rho = 775.26(25)$ MeV and $\Gamma_\rho = 149.1(8)$ MeV are

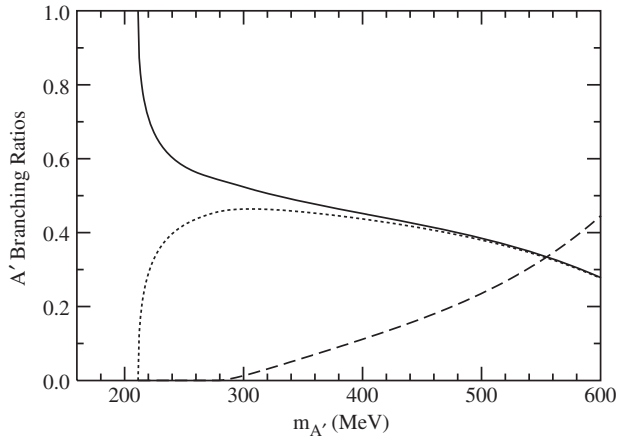

FIG. 3. The branching ratios for $\mathcal{B}(A' \to e^+e^-)$ (solid), $\mathcal{B}(A' \to \mu^+\mu^-)$ (dotted), and $\mathcal{B}(A' \to \pi^+\pi^-)$ (dashed) as per Eqs. (18), (23), and (27), assuming that decays to the hidden sector do not occur, as a function of the A' mass in GeV.

reported. We employ this latter set of parameters in our analysis here, and the incurred differences are negligible. We display the resulting A' branching ratios in Fig. 3, and the results are similar, though our $\Gamma(A' \to \pi^+\pi^-)$ is a bit larger than those determined using the prescription of Eq. (24) [52].

1. On $\Gamma(A' \to \text{hadrons})$ at higher energies

The proton initial-state radiation mechanism for dark gauge boson production can probe A' masses much in excess of 600 MeV, so that we now develop an expression for $\Gamma(A' \to \pi^+\pi^-)$, as well as for $\Gamma(A' \to \text{hadrons})$, in this mass region. To go beyond the prescription of Eq. (24) in estimating $\Gamma(A' \to \text{hadrons})$, we use Eq. (26) at $s = m_{A'}^2$ to rewrite Eq. (23) as

$$\Gamma(A' \to \pi^+\pi^-) = \frac{1}{3}\varepsilon^2\alpha m_{A'}\left(1 - 4\frac{M_\mu^2}{m_{A'}^2}\right)^{1/2} \times \left(1 + 2\frac{M_\mu^2}{m_{A'}^2}\right)\mathcal{R}(m_{A'}^2), \tag{28}$$

which is some 10% smaller than Eq. (24) if $m_{A'} = 300$ MeV. For $m_{A'}$ in excess of the $\pi\omega$ threshold, or ≈920 MeV, Eq. (28) is simply that of $\Gamma(A' \to \text{hadrons})$, implying that $\mathcal{B}(A' \to e^+e^-) + \mathcal{B}(A' \to \mu^+\mu^-) + \mathcal{B}(A' \to \pi^+\pi^-) < 1$ as well.

2. On $\Gamma(A' \to \text{invisibles})$

It is entirely possible that a produced dark gauge boson also decays invisibly to the particles of the hidden sector, though this possibility has been neglected in early studies [37]. Nevertheless, it can readily be incorporated, both in this case and throughout, by making the total visible decay width some fixed fraction of the total width. Varying the fraction of decays to the invisible sector consequently changes the exclusion plot.

D. The decay $\eta \to \gamma\rho' \to \gamma\pi^+\pi^-$

Now we turn to the possibility of a dark gauge boson, the ρ', which may or may not be a composite object. To anchor our analysis we first compute the rate for $\eta(p) \to \gamma(k)\pi^+(p_2)\pi^-(p_1)$ in the SM, where we assume, in analogy to our earlier work, that the decay vertex is mediated by the axial anomaly in the low-energy chiral theory of hadrons [152,153], where we refer to Ref. [139] for an analysis of this assertion within chiral perturbation theory. In particular, we assume that the decay is dominated by the $\eta \to (\pi\pi)_{L=1}\gamma$ channel, with the ρ playing a prominent role. Since $\rho \to \pi^+\pi^-$ is a p-wave decay, we define the coupling g_ρ as per

$$\langle \pi^+(p_2)\pi^-(p_1)|\rho^0(p_\rho, \varepsilon_\rho)\rangle = -g_\rho \varepsilon_\rho \cdot (p_2 - p_1) \tag{29}$$

to yield the decay amplitude

$$\mathcal{M} = -\frac{A_\eta}{2}\varepsilon_{\mu\nu\rho\sigma}\varepsilon^{\mu *}(k)\varepsilon_\rho^{\nu *}(p_\rho)k^\rho p_\rho^\sigma \frac{f_{\rho\gamma} g_\rho \varepsilon_\rho \cdot (p_2 - p_1)}{s - M_\rho^2 + i\Pi(s)}, \tag{30}$$

where $s = p_\rho^2$, and $\Pi(s)$ is defined after Eq. (27). Summing over the ρ spin, this becomes

$$\mathcal{M} = -A_\eta \varepsilon_{\mu\nu\rho\sigma}\varepsilon^{\mu *}(k) p_1^\nu k^\rho p_2^\sigma \frac{f_{\rho\gamma} g_\rho}{s - M_\rho^2 + i\Pi(s)}. \tag{31}$$

We note that this is just a special case of $\mathcal{M} = \varepsilon_{\mu\nu\rho\sigma}\varepsilon^{\mu *} p_1^\nu k^\rho p_2^\sigma P(s) F_\pi(s)$, where $P(s)$ is a polynomial of form $P(s) = A_\eta(1 + \alpha s)$ [154]. The corrections to this framework in $\eta \to \pi^+\pi^-\gamma$ decay are very small [154–156], supporting its use in the analysis here. Evaluating the integral over the three-body phase space (with the integral over solid angle computed in the rest frame of the $\pi^+\pi^-$ pair) yields

$$\Gamma(\eta \to \gamma\pi^+\pi^-) = \frac{M_\eta^7 |A_\eta|^2}{3\pi^3 2^{11}} \int_{r^2}^1 dx x(1-x)^3 \left(\sqrt{1 - r^2/x}\right)^3 \times |F_\pi(xM_\eta^2)|^2 (P_\eta(xM_\eta^2))^2, \tag{32}$$

where $r = 2M_\pi/M_\eta$, $x = s/M_\eta^2$, and we have included the polynomial of Ref. [154] as $P_\eta(s) = 1 + \alpha s$, with $\alpha = (1.96(27)_{\text{stat}}(2)_{\text{sys}})\text{GeV}^{-2}$ [154]. Although we could determine the constant A_η by simply appealing to the empirical $\eta \to \gamma\pi^+\pi^-$ partial width, it is worth noting that the axial anomaly can fix this constant as well. That is, the low-energy theorem relating $\gamma^* \to \pi^+\pi^-\pi^0$ to $\pi^0 \to \gamma\gamma$ [157–159] generalizes in the chiral $\text{SU}(3)_f$ limit at zero

momenta to yield $A_\eta = e/(4\sqrt{3}\pi^2 f_\pi^3)$ [160,161]. Using $f_\pi = 92.2$ MeV, this yields $A_\eta = 5.65\ \mathrm{GeV}^{-3}$, whereas including $\mathrm{SU}(3)_f$ breaking and $\eta - \eta'$ mixing gives an additional multiplicative factor of $\xi = \cos\theta f_\pi/f_8 - \sin\theta\sqrt{2}f_\pi/f_0$ [160,161], which evaluates to $\xi = 1.057$ using $f_8/f_\pi = 1.3$, $f_0/f_\pi = 1.04$, and $\theta = -20°$ [160,161]. Doing the integral in Eq. (32) using Eq. (27), $A_\eta = 5.65\ \mathrm{GeV}^{-3}$, and $\Gamma_{\mathrm{tot}} = 1.31(5)$ keV [140] yields a branching ratio of 6.42%, whereas the experimental result is $\mathcal{B}(\eta \to \pi^+\pi^-\gamma) = (4.22(8))\%$ [140], a fractional difference of some 30%. Including ξ and an overall correction factor to A_η of $(1+\delta)$ with $\delta = -0.22(4)$ from the assessment of Ref. [154] yields $\mathcal{B}(\eta \to \pi^+\pi^-\gamma) = 4.37\%$, in reasonable agreement with experiment given the various uncertainties. To adapt this framework to the computation of $\Gamma(\eta \to \gamma\rho' \to \gamma\pi^+\pi^-)$, we need only replace $(s - M_\rho^2)^2 + \Pi^2(s)$ in Eq. (27) with $(s - M_{\rho'}^2)^2 + M_{\rho'}^2\Gamma_{\rho'}^2$ and multiply by ε^4. Although $\mathcal{B}(\rho' \to \pi^+\pi^-)$ could plausibly be less than 1, we shall assume that it is still reasonable to use the narrow width approximation of Eq. (15), yielding

$$\begin{aligned}\Gamma(\eta \to \gamma\rho' \to \gamma\pi^+\pi^-) &= \frac{\varepsilon^4}{3\pi^2 2^{11}} M_\eta^3 |A_\eta(1+\delta)|^2 \frac{M_{\rho'}}{\Gamma_{\rho'}} \\ &\times P_\eta^2(M_{\rho'}^2) f_{\rho\gamma}^2 g_\rho^2 \left(1 - \frac{M_{\rho'}^2}{M_\eta^2}\right)^3 \left(1 - \frac{4M_\pi^2}{M_{\rho'}^2}\right)^{3/2}. \end{aligned} \tag{33}$$

Supposing a ρ' coupling of the form given in Eq. (29), but with strength $g_\rho\varepsilon$, we have

$$\Gamma(\rho' \to \pi^+\pi^-) = \frac{1}{48\pi}\varepsilon^2 g_\rho^2 M_{\rho'} \left(1 - \frac{4M_\pi^2}{M_{\rho'}^2}\right)^{3/2}. \tag{34}$$

Thus, if $\Gamma_{\rho'} = \Gamma(\rho' \to \pi^+\pi^-)$, we find

$$\begin{aligned}\Gamma(\eta \to \gamma\rho') = \frac{\varepsilon^2}{128\pi} M_\eta^3 |A_\eta(1+\delta)|^2 P_\eta^2(M_{\rho'}^2) f_{\rho\gamma}^2 \\ \times \left(1 - \frac{M_{\rho'}^2}{M_\eta^2}\right)^3. \end{aligned} \tag{35}$$

In what follows, we include the possibility of invisible decays by studying the impact of making $\mathcal{B}(\rho' \to \pi^+\pi^-)$ some definite fraction less than 1 on the parameter exclusion plot.

IV. EXPERIMENTAL PROSPECTS

Already, there are a large number of searches for dark photons and a number of planned searches [37,40–52,54–57,59–66].

We illustrate here a possible new search for dark photons at the FNAL E906 (SeaQuest) experiment at Fermilab. This experiment was designed to perform a measurement of Drell-Yan processes for a proton beam incident on stationary targets. The experiment is comprised of an intense (5×10^{12} protons/spill at 1 spill per min) 120 GeV proton beam incident on a target. Less than a meter downstream of the target is a 5 m–long solid iron magnet that not only serves to begin the analysis of the muon pair from the Drell-Yan process, but also serves as a beam dump. This beam dump tremendously attenuates all hadrons and most charged particles from the target with the exception of muons. Following the solid iron magnet, there are two stations of scintillator hodoscopes and drift chambers that can define the vertex of either a prompt Drell-Yan event in the target or beam dump or from the decay of a prompt or displaced vertex from a dark photon. The first detector station is followed by an air gap magnet and two additional detector stations. This system serves as the pair spectrometer and can measure the mass of an event with a relative mass resolution that varies between 2.5% and 6% depending on where the event occurs in the solid iron magnet. A 1 m–thick block of iron was placed just upstream of the fourth detector station and serves to filter most charged particles except muons. The fourth detector substation comprises a layer of proportional tubes and scintillator paddles that serve as a muon identification system. A schematic overview of the SeaQuest spectrometer is shown in Fig. 1 [36].

Clearly, experiment E906 has all the basic elements of a "shining-through-the-wall" beam-stop experiment to search for dark photons. The basic elements consist of a high-energy proton beam incident on a fixed target and a pair spectrometer which detects lepton pairs from the decay of the dark photon, where the spectrometer is well shielded from the target in order to minimize background events from ordinary SM processes. Consequently, the dark photons, being weakly interacting, can travel unscathed through the shield, where they decay into lepton pairs and are subsequently detected in the pair spectrometer.

We have been conservative in the following simulations. We have only considered events where the background is known to be low, namely after all or most of the shield. For the special case of muon pair detection, we have used part of the last meter of the Fe shield as part of the fiducial region, since the Fe absorber has little effect on the muons. As more is known about the experiment and if more trigger optimization can be implemented, it may be possible to extend the fiducial region further upstream in the beam dump. However, such studies are beyond the scope of this work.

A. η meson decay to charged lepton pairs

Here we illustrate the regions of sensitivity in the parameter space of ε and dark photon mass $m_{A'}$ for

SeaQuest for four different processes that could be used to search for dark photons. Figure 2 shows the projected regions of sensitivity for SeaQuest along with areas excluded by electron and proton beam dump experiments and proposed experiments. The simulation assumes that we have a 200-day experiment with an overall efficiency of about 30%, which approximates the conditions experienced in the experiment thus far. We investigated dark photon production from radiative η and π^0 decays and proton bremsstrahlung. The η and π^0 yields per proton have been estimated from GEANT4 simulations that record the energy and transverse momentum spectra of η and π^0 mesons produced (shown in Figs. 4 and 5) when 6.2×10^6 protons at 120 GeV are incident on a 4.75 m–long Fe beam dump. These energy and p_T distributions were used in the calculation of the estimation of the dark photon yield.

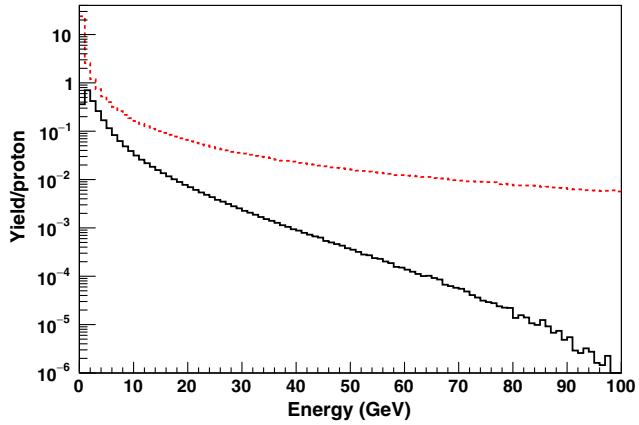

FIG. 4. The η (solid) and π^0 (dotted) yield/proton as a function of the energy of the particles as obtained from GEANT4 Monte Carlo simulations of 120 GeV protons interacting with the Fe beam dump.

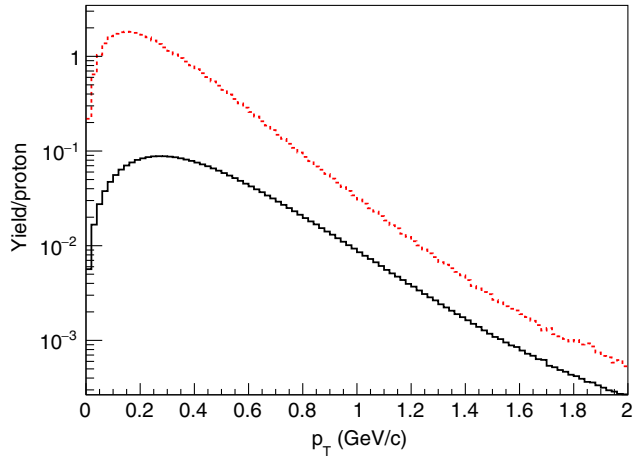

FIG. 5. The η (solid) and π^0 (dotted) yield/proton as a function of the transverse momentum p_T obtained from GEANT4 Monte Carlo simulations of 120 GeV protons interacting with the Fe beam dump.

In this projection, we assume that the fiducial region for detecting the decay of the dark photons to a muon pair begins 4 m downstream of the front edge of the beam stop and extends 0.85 m downstream. This fiducial region ensures that all decay muons must travel through at least 0.15 m of FMAG, which would impart an effective p_T kick of about 0.08 GeV. This ensures that the muon pair would be well separated before reaching the first detector station. For the decay of an e^+e^- pair, or in later discussion, a pion pair, the fiducial region is only 0.95 m and entirely outside the Fe magnet. For the case of e^+e^- or $\pi^+\pi^-$ pairs, it might be necessary to add a small air gap magnet between the downstream end of FMAG and the first detector station to ensure a small p_T kick. For the purpose of simulation, it was assumed that the necessary separation of the pairs was met. To be specific, the expression used for the A' decays to lepton pairs in the fiducial length, $l_{\rm fid}$, after the A' traverses the length of the beam dump, $l_{\rm dump}$, is given by

$$N_{\rm dec} = N_0 \mathcal{B}(A' \to \ell^+\ell^-) \exp\left(-\frac{l_{\rm dump}}{c\tau_{A'}}\frac{m_{A'}}{|\mathbf{p}_{A'}|}\right) \times \left[1 - \exp\left(-\frac{l_{\rm fid}}{c\tau_{A'}}\frac{m_{A'}}{|\mathbf{p}_{A'}|}\right)\right], \quad (36)$$

where $\mathbf{p}_{A'}$ is the A' momentum in the laboratory frame, and $\tau_{A'}$ is the A' lifetime in the A' rest frame.

Two different approaches were used to determine the acceptance of the spectrometer for a dark photon. They both assumed a dark photon of various masses decaying at different vertex positions in the beam stop. The first method makes use of the full spectrometer geometry in a GEANT4 (version 4.9.6.p03 [162]) simulation. The second method uses the spectrometer geometry in a simplified situation where multiple scattering and energy loss of the decay particles are put in explicitly. The kinematic variables and the dimuon yields were compared, and there is good agreement between the two approaches. Currently, our acceptance is limited by the decay length of the dark photon. Once track reconstruction is optimized and a detailed simulation of the background events is achieved, it may be possible to probe larger values in ε parameter space.

The projected regions of sensitivity based on this simulation are indicated in Fig. 6. The contours shown in the figure indicate ten-event contours, which should be adequate to set 95% confidence levels on exclusion of dark photons. For example, if we assume a signal of 10 events and a detected number of events of 10 with a background of 7 events, the confidence level [163] that the true number of events is less than 10 is 94.6%. Three cases are displayed: (1) detection of a muon pair from η decay to a dark photon and subsequent A' decay to a muon pair, (2) detection of an e^+e^- pair from η decay and subsequent A' decay, and (3) detection of e^+e^- decay from neutral pion decay and

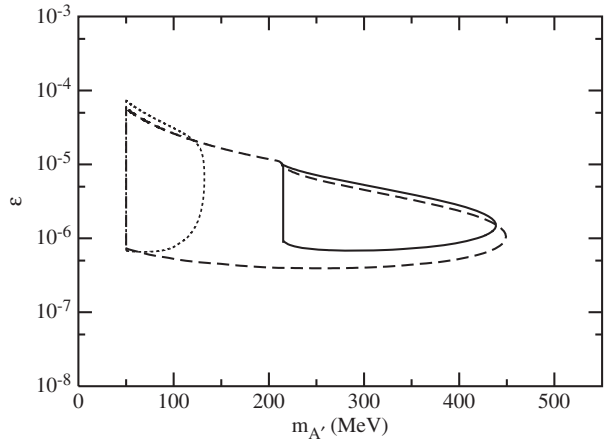

FIG. 6. Preliminary projections for an η meson decaying to a photon (γ) and a dark photon, denoted by A'. The A' can subsequently decay into a $\mu^+\mu^-$ pair (solid) or an e^+e^- pair (dashed). Here decays to the hidden sector do not occur. The dotted curve represents the projected exclusion limit for π^0 decay.

subsequent A' decay. It is assumed that there are no decays to the invisible sector for the projections of Fig. 6.

Many projections and exclusion plots assume that the decay to the visible sector is 100%. In Fig. 7 we explore the case where A' decay to the invisible sector is also allowed to determine its impact on the ability to limit the A'. The figure shows the specific case of η decay to $\gamma A'$, followed by $A' \to \mu^+\mu^-$. Furthermore, it is assumed that the branching ratio to the hidden sector, $\mathcal{B}(A' \to \text{invisibles})$, varies from 0% to 90%. Clearly, if decay to the hidden sector is permitted, the region excluded by the experiments dramatically shrinks.

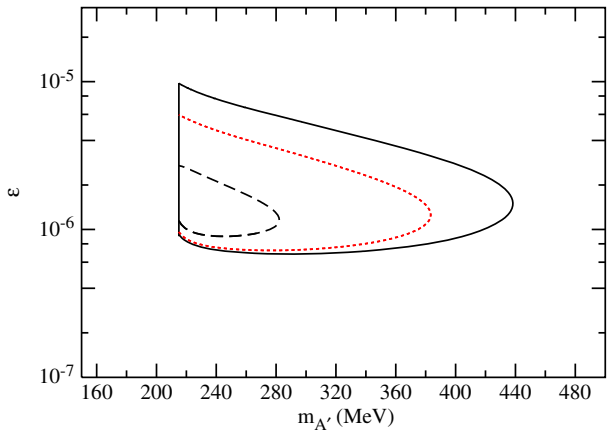

FIG. 7. Here the A' is produced by η decay. The A' subsequently decays to a muon pair. The preliminary projected exclusion regions for SeaQuest for three branching ratios to the dark sector between 0% and 90% are shown. Specifically, $\mathcal{B}(A' \to \text{invisibles}) = 0,\ 0.70,\ 0.90$, which are shown as solid, dotted, and dashed curves, respectively.

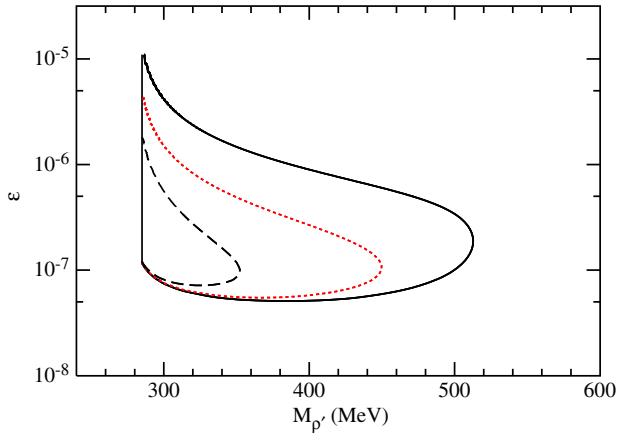

FIG. 8. Preliminary projections for an η meson decaying to a photon and a dark gauge boson ρ' that couples to quarks, with a probability governed by the square of the coupling constant between light and dark sectors of ε^2 with the probability governed by Eq. (35). The ρ' can subsequently decay into a charged pion pair with a decay lifetime proportional to ε^{-2} governed by Eq. (34). The ρ' is permitted to decay to the dark sector with a branching ratio of $\mathcal{B}(\rho' \to \text{invisibles}) = 0,\ 0.80,\ 0.95$, which are shown as solid, dotted, and dashed curves, respectively.

B. η meson decay to a charged pion pair

With relatively small modifications, it may be possible for the pair spectrometer associated with the SeaQuest experiment to detect a charged pion pair. Although the detectors in this spectrometer presently do not have the capability to distinguish between an e^+e^- pair and a pion pair, it may not be necessary in a first stage of the experiment. If a mass peak is observed from a displaced vertex in the SeaQuest experiment, then the necessary particle identification could be added to the detector to determine whether the pair is leptonic or hadronic. If we consider η decay to a photon and a dark ρ', and the dark ρ' subsequently decays to a pion pair, the expected sensitivity plot is given in Fig. 8, again showing ten-event contours based on Eqs. (35) and (34). The effect of the ρ' decay to the invisible sector has also been explored in the figure.

V. SUMMARY AND OUTLOOK

In this paper we have explored the discovery prospects of the SeaQuest experiment, E906 at Fermilab, operated in proton beam dump mode. We have explored the ability to which it can explore new regions of dark photon parameter space, and how, if pion pair detection were made possible, it can search for an entirely new kind of hidden sector, one probed through the hidden strong interactions of quarks. The latter scenario has never been explored in beam dump experiments, and the possibility of strongly coupled hidden sectors at sub-GeV mass scales is poorly constrained by other considerations [111]. We emphasize that the SeaQuest projections in this paper have been computed assuming one

year of running with a nonoptimized detector. Increasing the exposure could lower the epsilon range considerably, and, in the case of the proton bremsstrahlung mechanism, permit sensitivity to higher-mass gauge bosons as well.

Moreover, the prospect of polarized proton beams [127] opens a unique window of sensitivity to light Z' gauge bosons, to the Z_d scenario of Refs. [68,85,94,95] and, in the event of $\pi^+\pi^-$ detection, to the leptophobic light Z' proposed in Ref. [111]. Increasing either the proton beam energy or the length of the fiducial region in the iron beam stop can also extend the sensitivity of SeaQuest to heretofore unexplored regions of hidden-sector parameter space.

ACKNOWLEDGMENTS

We greatly appreciate the assistance of M. M. Medeiros and B. Nadim with GEANT4 Monte Carlo simulations. We are grateful for useful discussions with C. Brown, D. Geesaman, P. Reimer, R. Gilman, J.-C. Peng, R. Essig, J. Blümlein, J. Brunner, and J. Qian. We are also grateful to P. Masjuan for helpful correspondence. This work was supported by Department of Energy (DOE), Office of Science, Office of Nuclear Physics, Contracts No. DE-FG02-96ER40989 (S. G.) and No. DE-AC02-06CH11357 (R. H.), and by National Science Foundation (NSF) Grant No. NSF PHY 1306126 (A.T).

[1] M. J. G. Veltman, Acta Phys. Pol. B **8**, 475 (1977).
[2] L. Susskind, Phys. Rev. D **20**, 2619 (1979).
[3] H. Baer and X. Tata, *Weak Scale Supersymmetry: From Superfields to Scattering Events* (Cambridge University Press, Cambridge, England 2006).
[4] G. Bertone, D. Hooper, and J. Silk, Phys. Rep. **405**, 279 (2005).
[5] J. L. Feng, Annu. Rev. Astron. Astrophys. **48**, 495 (2010).
[6] S. Gardner and G. Fuller, Prog. Part. Nucl. Phys. **71**, 167 (2013).
[7] G. Jungman, M. Kamionkowski, and K. Griest, Phys. Rep. **267**, 195 (1996).
[8] A. Birkedal, A. Noble, M. Perelstein, and A. Spray, Phys. Rev. D **74**, 035002 (2006).
[9] S. B. Gudnason, C. Kouvaris, and F. Sannino, Phys. Rev. D **74**, 095008 (2006).
[10] D. Hooper and S. Profumo, Phys. Rep. **453**, 29 (2007).
[11] L. B. Okun, Zh. Eksp. Teor. Fiz. **83**, 892 (1982) [Sov. Phys. JETP **56**, 502 (1982)].
[12] P. Sikivie, Phys. Rev. Lett. **51**, 1415 (1983); **52**, 695(E) (1984).
[13] J. E. Moody and F. Wilczek, Phys. Rev. D **30**, 130 (1984).
[14] B. Holdom, Phys. Lett. B **178**, 65 (1986).
[15] R. Foot, A. Yu. Ignatiev, and R. R. Volkas, Phys. Lett. B **503**, 355 (2001).
[16] B. A. Dobrescu and I. Mocioiu, J. High Energy Phys. 11 (2006) 005.
[17] M. Ahlers, H. Gies, J. Jaeckel, J. Redondo, and A. Ringwald, Phys. Rev. D **76**, 115005 (2007).
[18] M. Ahlers, H. Gies, J. Jaeckel, J. Redondo, and A. Ringwald, Phys. Rev. D **77**, 095001 (2008).
[19] J. L. Feng and J. Kumar, Phys. Rev. Lett. **101**, 231301 (2008).
[20] A. Kusenko, Phys. Rep. **481**, 1 (2009).
[21] J. L. Feng, arXiv:1002.3828.
[22] R. Foot, A. Kobakhidze, and R. R. Volkas, Phys. Rev. D **82**, 035005 (2010).
[23] M. Le Dall, M. Pospelov, and A. Ritz, Phys. Rev. D **92**, 016010 (2015).
[24] N. Arkani-Hamed, D. P. Finkbeiner, T. R. Slatyer, and N. Weiner, Phys. Rev. D **79**, 015014 (2009).
[25] I. Cholis, L. Goodenough, D. Hooper, M. Simet, and N. Weiner, Phys. Rev. D **80**, 123511 (2009).
[26] P. J. Fox and E. Poppitz, Phys. Rev. D **79**, 083528 (2009).
[27] D. Hooper and L. Goodenough, Phys. Lett. B **697**, 412 (2011).
[28] M. Pospelov, Phys. Rev. D **80**, 095002 (2009).
[29] P. Fayet, Nucl. Phys. **B187**, 184 (1981).
[30] S. N. Gninenko and N. V. Krasnikov, Phys. Lett. B **513**, 119 (2001).
[31] P. Fayet, Phys. Rev. D **75**, 115017 (2007).
[32] C. Boehm, P. Fayet, and J. Silk, Phys. Rev. D **69**, 101302 (2004).
[33] T. Appelquist and J. Carazzone, Phys. Rev. D **11**, 2856 (1975).
[34] W. Buchmuller and D. Wyler, Nucl. Phys. **B268**, 621 (1986).
[35] B. Grzadkowski, M. Iskrzynski, M. Misiak, and J. Rosiek, J. High Energy Phys. 10 (2010) 085.
[36] L. D. Isenhower *et al.*, Fermilab Report No. FERMILAB-PROPOSAL-0906, 2001.
[37] J. D. Bjorken, R. Essig, P. Schuster, and N. Toro, Phys. Rev. D **80**, 075018 (2009).
[38] B. Batell, M. Pospelov, and A. Ritz, Phys. Rev. D **80**, 095024 (2009).
[39] B. Batell, M. Pospelov, and A. Ritz, Phys. Rev. D **79**, 115008 (2009).
[40] J. D. Bjorken, S. Ecklund, W. R. Nelson, A. Abashian, C. Church, B. Lu, L. W. Mo, T. A. Nunamaker, and P. Rassmann, Phys. Rev. D **38**, 3375 (1988).
[41] E. M. Riordan *et al.*, Phys. Rev. Lett. **59**, 755 (1987).
[42] A. Bross, M. Crisler, S. H. Pordes, J. Volk, S. Errede, and J. Wrbanek, Phys. Rev. Lett. **67**, 2942 (1991).
[43] S. N. Gninenko, Phys. Rev. D **85**, 055027 (2012).
[44] S. N. Gninenko, Phys. Lett. B **713**, 244 (2012).
[45] S. Abrahamyan *et al.*, Phys. Rev. Lett. **107**, 191804 (2011).
[46] F. Archilli *et al.*, Phys. Lett. B **706**, 251 (2012).
[47] J. Batley *et al.*, Phys. Lett. B **746**, 178 (2015).

[48] A. Adare *et al.* (PHENIX Collaboration), Phys. Rev. C **91**, 031901 (2015).
[49] H. Merkel *et al.* (A1 Collaboration), Phys. Rev. Lett. **106**, 251802 (2011).
[50] J. Lees (*BABAR* Collaboration), Phys. Rev. Lett. **113**, 201801 (2014).
[51] J. Blümlein and J. Brunner, Phys. Lett. B **701**, 155 (2011).
[52] J. Blümlein and J. Brunner, Phys. Lett. B **731**, 320 (2014).
[53] S. Gninenko, Phys. Rev. D **87**, 035030 (2013).
[54] G. Aad *et al.* (ATLAS Collaboration), J. High Energy Phys. 11 (2014) 088.
[55] G. Aad *et al.* (ATLAS Collaboration), Phys. Rev. D **92**, 072004 (2015).
[56] J. D. Bjorken, R. Essig, R. Schuster, N. Toro, B. Wojtsekhowski *et al.*, [The A' Experiment (APEX)], Reports No. PR-10-009, No. E12-10-009, 2010.
[57] A. Grillo*et al.* (Heavy Photon Search (HPS) Collaboration), Jefferson Lab Report No. E11-006, 2011.
[58] N. Baltzell (private communication).
[59] M. Freytsis, G. Ovanesyan, and J. Thaler, J. High Energy Phys. 01 (2010) 111.
[60] B. Wojtsekhowski, D. Nikolenko, and I. Rachek, arXiv: 1207.5089.
[61] T. Beranek, H. Merkel, and M. Vanderhaeghen, Phys. Rev. D **88**, 015032 (2013).
[62] S. Gninenko, Phys. Rev. D **89**, 075008 (2014).
[63] S. Andreas *et al.*, arXiv:1312.3309.
[64] B. Echenard, R. Essig, and Y.-M. Zhong, J. High Energy Phys. 01 (2015) 113.
[65] S. Alekhin, W. Altmannshofer, T. Asaka, B. Batell, F. Bezrukov *et al.*, arXiv:1504.04855.
[66] P. Ilten, J. Thaler, M. Williams, and W. Xue, Phys. Rev. D **92**, 115017 (2015).
[67] G. Agakishiev *et al.* (HADES Collaboration), Phys. Lett. B **731**, 265 (2014).
[68] H. Davoudiasl, H.-S. Lee, and W. J. Marciano, Phys. Rev. D **89**, 095006 (2014).
[69] R. Essig, R. Harnik, J. Kaplan, and N. Toro, Phys. Rev. D **82**, 113008 (2010).
[70] C. Athanassopoulos *et al.* (LSND Collaboration), Phys. Rev. C **58**, 2489 (1998).
[71] J. B. Dent, F. Ferrer, and L. M. Krauss, arXiv:1201.2683.
[72] H. K. Dreiner, J.-F. Fortin, C. Hanhart, and L. Ubaldi, Phys. Rev. D **89**, 105015 (2014).
[73] A. Fradette, M. Pospelov, J. Pradler, and A. Ritz, Phys. Rev. D **90**, 035022 (2014).
[74] R. Foot and S. Vagnozzi, Phys. Rev. D **91**, 023512 (2015).
[75] D. Kazanas, R. N. Mohapatra, S. Nussinov, V. L. Teplitz, and Y. Zhang, Nucl. Phys. **B890**, 17 (2014).
[76] L. Barabash, S. Baranov, Y. Batusov, S. Bunyatov, O. Denisov *et al.*, Phys. Lett. B **295**, 154 (1992).
[77] D. E. Kaplan, M. A. Luty, and K. M. Zurek, Phys. Rev. D **79**, 115016 (2009).
[78] H. Davoudiasl and R. N. Mohapatra, New J. Phys. **14**, 095011 (2012).
[79] G. Servant and S. Tulin, Phys. Rev. Lett. **111**, 151601 (2013).
[80] J. L. Feng, M. Kaplinghat, H. Tu, and H.-B. Yu, J. Cosmol. Astropart. Phys. 07 (2009) 004.
[81] D. E. Kaplan, G. Z. Krnjaic, K. R. Rehermann, and C. M. Wells, J. Cosmol. Astropart. Phys. 05 (2010) 021.
[82] J. M. Cline, Z. Liu, and W. Xue, Phys. Rev. D **85**, 101302 (2012).
[83] J. Fan, A. Katz, L. Randall, and M. Reece, Phys. Rev. Lett. **110**, 211302 (2013).
[84] J. Fan, A. Katz, L. Randall, and M. Reece, Phys. Dark Univ. **2**, 139 (2013).
[85] H. Davoudiasl, H.-S. Lee, and W. J. Marciano, Phys. Rev. D **85**, 115019 (2012).
[86] B. Holdom, Phys. Lett. **166B**, 196 (1986).
[87] S. Davidson, S. Hannestad, and G. Raffelt, J. High Energy Phys. 05 (2000) 003.
[88] B.-A. Gradwohl and J. A. Frieman, Astrophys. J. **398**, 407 (1992).
[89] L. Ackerman, M. R. Buckley, S. M. Carroll, and M. Kamionkowski, Phys. Rev. D **79**, 023519 (2009).
[90] F.-Y. Cyr-Racine and K. Sigurdson, Phys. Rev. D **87**, 103515 (2013).
[91] J. M. Cline, Z. Liu, G. Moore, and W. Xue, Phys. Rev. D **89**, 043514 (2014).
[92] F.-Y. Cyr-Racine, R. de Putter, A. Raccanelli, and K. Sigurdson, Phys. Rev. D **89**, 063517 (2014).
[93] S. Gopalakrishna, S. Jung, and J. D. Wells, Phys. Rev. D **78**, 055002 (2008).
[94] H. Davoudiasl, H.-S. Lee, and W. J. Marciano, Phys. Rev. D **86**, 095009 (2012).
[95] H. Davoudiasl, H.-S. Lee, and W. J. Marciano, Phys. Rev. Lett. **109**, 031802 (2012).
[96] E. C. G. Stueckelberg, Helv. Phys. Acta **11**, 299 (1938).
[97] D. Feldman, Z. Liu, and P. Nath, Phys. Rev. D **75**, 115001 (2007).
[98] M. Baumgart, C. Cheung, J. T. Ruderman, L.-T. Wang, and I. Yavin, J. High Energy Phys. 04 (2009) 014.
[99] L. B. Okun, Pis'ma Zh. Eksp. Teor. Fiz. **31**, 156 (1979) [JETP Lett. **31**, 144 (1980)].
[100] L. B. Okun, Nucl. Phys. **B173**, 1 (1980).
[101] S. Gupta and H. R. Quinn, Phys. Rev. D **25**, 838 (1982).
[102] A. E. Nelson and N. Tetradis, Phys. Lett. B **221**, 80 (1989).
[103] S. Rajpoot, Phys. Rev. D **40**, 2421 (1989).
[104] R. Foot, G. C. Joshi, and H. Lew, Phys. Rev. D **40**, 2487 (1989).
[105] X.-G. He and S. Rajpoot, Phys. Rev. D **41**, 1636 (1990).
[106] C. D. Carone and H. Murayama, Phys. Rev. Lett. **74**, 3122 (1995).
[107] C. D. Carone and H. Murayama, Phys. Rev. D **52**, 484 (1995).
[108] A. Aranda and C. D. Carone, Phys. Lett. B **443**, 352 (1998).
[109] P. Fileviez Perez and M. B. Wise, Phys. Rev. D **82**, 011901 (2010); **82**, 079901(E) (2010).
[110] S. Tulin, Phys. Rev. D **89**, 114008 (2014).
[111] B. A. Dobrescu and C. Frugiuele, Phys. Rev. Lett. **113**, 061801 (2014).
[112] R. Machleidt, K. Holinde, and C. Elster, Phys. Rep. **149**, 1 (1987).
[113] K. Blum, R. T. D'Agnolo, M. Lisanti, and B. R. Safdi, Phys. Lett. B **737**, 30 (2014).
[114] Y. Hochberg, E. Kuflik, T. Volansky, and J. G. Wacker, Phys. Rev. Lett. **113**, 171301 (2014).
[115] Y. Hochberg, E. Kuflik, H. Murayama, T. Volansky, and J. G. Wacker, Phys. Rev. Lett. **115**, 021301 (2015).

[116] K. K. Boddy, J. L. Feng, M. Kaplinghat, and T. M. P. Tait, Phys. Rev. D **89**, 115017 (2014).
[117] R. M. Godbole, G. Mendiratta, and T. M. P. Tait, J. High Energy Phys. 08 (2015) 064.
[118] M. J. Strassler and K. M. Zurek, Phys. Lett. B **651**, 374 (2007).
[119] T. Han, Z. Si, K. M. Zurek, and M. J. Strassler, J. High Energy Phys. 07 (2008) 008.
[120] J. Kang and M. A. Luty, J. High Energy Phys. 11 (2009) 065.
[121] R. Harnik, G. D. Kribs, and A. Martin, Phys. Rev. D **84**, 035029 (2011).
[122] S. Gardner and D. He, Phys. Rev. D **87**, 116012 (2013).
[123] M. Bando, T. Kugo, S. Uehara, K. Yamawaki, and T. Yanagida, Phys. Rev. Lett. **54**, 1215 (1985).
[124] R. Kitano, J. High Energy Phys. 11 (2011) 124.
[125] U.-G. Meißner, Phys. Rep. **161**, 213 (1988).
[126] H. B. O'Connell, B. Pearce, A. W. Thomas, and A. G. Williams, Prog. Part. Nucl. Phys. **39**, 201 (1997).
[127] L. D. Isenhower *et al.*, Fermilab Report No. FERMILAB-PROPOSAL-1027, 2012.
[128] J.-C. Peng and S. Prasad (private communication).
[129] H. Leutwyler and M. A. Shifman, Nucl. Phys. **B343**, 369 (1990).
[130] J. F. Donoghue, J. Gasser, and H. Leutwyler, Nucl. Phys. **B343**, 341 (1990).
[131] S. L. Adler, Phys. Rev. **177**, 2426 (1969).
[132] J. Bell and R. Jackiw, Nuovo Cimento A **60**, 47 (1969).
[133] S. L. Adler and W. A. Bardeen, Phys. Rev. **182**, 1517 (1969).
[134] R. Dalitz, Proc. Phys. Soc. London Sect. A **64**, 667 (1951).
[135] K. Mikaelian and J. Smith, Phys. Rev. D **5**, 1763 (1972).
[136] K. Kampf, M. Knecht, and J. Novotny, Eur. Phys. J. C **46**, 191 (2006).
[137] P. Masjuan, Phys. Rev. D **86**, 094021 (2012).
[138] M. Hoferichter, B. Kubis, S. Leupold, F. Niecknig, and S. P. Schneider, Eur. Phys. J. C **74**, 3180 (2014).
[139] J. Bijnens, A. Bramon, and F. Cornet, Z. Phys. C **46**, 599 (1990).
[140] K. Olive *et al.* (Particle Data Group), Chin. Phys. C **38**, 090001 (2014).
[141] P. Masjuan (private communication).
[142] G. P. Lepage and S. J. Brodsky, Phys. Lett. **87B**, 359 (1979).
[143] R. Escribano, P. Masjuan, and P. Sanchez-Puertas, Eur. Phys. J. C **75**, 414 (2015).
[144] P. Aguar-Bartolome *et al.* (A2 Collaboration), Phys. Rev. C **89**, 044608 (2014).
[145] R. Escribano, P. Masjuan, and P. Sanchez-Puertas, Phys. Rev. D **89**, 034014 (2014).
[146] H. Berghäuser *et al.*, Phys. Lett. B **701**, 562 (2011).
[147] D. Babusci *et al.* (KLOE-2 Collaboration), J. High Energy Phys. 01 (2013) 119.
[148] S. Gardner and H. B. O'Connell, Phys. Rev. D **57**, 2716 (1998).
[149] D. Boutigny *et al.* (*BABAR* Collaboration), http://slac.stanford.edu/pubs/slacreports/reports19/slac-r-504.pdf.
[150] S. Gardner and U.-G. Meißner, Phys. Rev. D **65**, 094004 (2002).
[151] S. Gardner and H. B. O'Connell, Phys. Rev. D **59**, 076002 (1999).
[152] J. Wess and B. Zumino, Phys. Lett. **37B**, 95 (1971).
[153] E. Witten, Nucl. Phys. **B223**, 422 (1983).
[154] F. Stollenwerk, C. Hanhart, A. Kupść, U.-G. Meißner, and A. Wirzba, Phys. Lett. B **707**, 184 (2012).
[155] C. Hanhart, A. Kupść, U.-G. Meißner, F. Stollenwerk, and A. Wirzba, Eur. Phys. J. C **73**, 2668 (2013).
[156] B. Kubis and J. Plenter, Eur. Phys. J. C **75**, 283 (2015).
[157] S. L. Adler, B. W. Lee, S. B. Treiman, and A. Zee, Phys. Rev. D **4**, 3497 (1971).
[158] R. Aviv and A. Zee, Phys. Rev. D **5**, 2372 (1972).
[159] M. V. Terent'ev, Phys. Lett. **38B**, 419 (1972).
[160] E. P. Venugopal and B. R. Holstein, Phys. Rev. D **57**, 4397 (1998).
[161] B. R. Holstein, Phys. Scripta **T99**, 55 (2002).
[162] https://geant4.web.cern.ch/geant4.
[163] G. Zech, Nucl. Instrum. Methods Phys. Res., Sect. A **277**, 608 (1989).